



State-of-the-Art Quantitative Assessment of Myocardial Ischemia by Stress Perfusion Cardiac Magnetic Resonance

Thiago Quinaglia, MD, PhD^a, Michael Jerosch-Herold, PhD^b,
Otávio R. Coelho-Filho, MD, PhD, MPH^{a,c,*}

KEYWORDS

- Myocardial ischemia • Cardiac magnetic resonance and stress perfusion
- Cardiovascular magnetic resonance • Myocardial perfusion • Quantitative ischemia assessment

KEY POINTS

- Cardiac magnetic resonance (CMR) provides excellent temporal and spatial resolution without the limitations associated with unfavorable echocardiographic windows, and low temporal and spatial resolution in nuclear medicine studies, nor does it involve ionizing radiation.
- Myocardial perfusion by CMR can be integrated with a spatially registered interrogation of regional function (wall thickening, segmental contractility, and myocardial deformation image), edema, fibrosis, and viability.
- These simultaneous faculties are not present in other imaging modalities.

INTRODUCTION

Cardiac magnetic resonance (CMR) has arisen as a method of choice for myocardial ischemia assessment. CMR is endowed with a series of advantageous characteristics, which are only in part present with other modalities. Although arguably still not the gold-standard method, stress perfusion CMR permits excellent spatial and temporal resolution, evaluation of contractile function (wall motility and thickening) and myocardial perfusion quantification, in addition to

assessment of myocardial viability and scar with late gadolinium enhancement (LGE) technique.¹ Moreover, multicenter studies^{2–5} have demonstrated outstanding sensitivity and specificity in the detection of significant coronary artery disease (CAD) in patients submitted to perfusion imaging during pharmacologic stress by CMR. A compilation of 26 studies,⁶ comprising more than 11,000 patients, predicted sensitivity of 89% and specificity of 80% in the detection of CAD by the stress perfusion of CMR (Fig. 1).

Disclosures: The authors have nothing to disclose.

^a Faculdade de Ciências Médicas, Universidade Estadual de Campinas, Rua Tessália Viera de Camargo, 126 - Cidade Universitária "Zeferino Vaz", Campinas, São Paulo 13083-887, Brazil; ^b Noninvasive Cardiovascular Imaging Program, Department of Radiology, Brigham and Women's Hospital, 75 Francis Street, Room L1-RA050, Mailbox #22, Boston, MA 02115, USA; ^c Department of Internal Medicine, Hospital das Clínicas, State University of Campinas, UNICAMP, Rua Vital Brasil, 251- Cidade Universitária "Zeferino Vaz", Campinas, São Paulo 13083-888, Brazil

* Corresponding author. Department of Internal Medicine, Hospital das Clínicas, State University of Campinas, UNICAMP, Rua Vital Brasil, 251- Cidade Universitária "Zeferino Vaz", Campinas, São Paulo 13083-888, Brazil.
E-mail addresses: orcfilho@unicamp.br; tavicocoelho@gmail.com

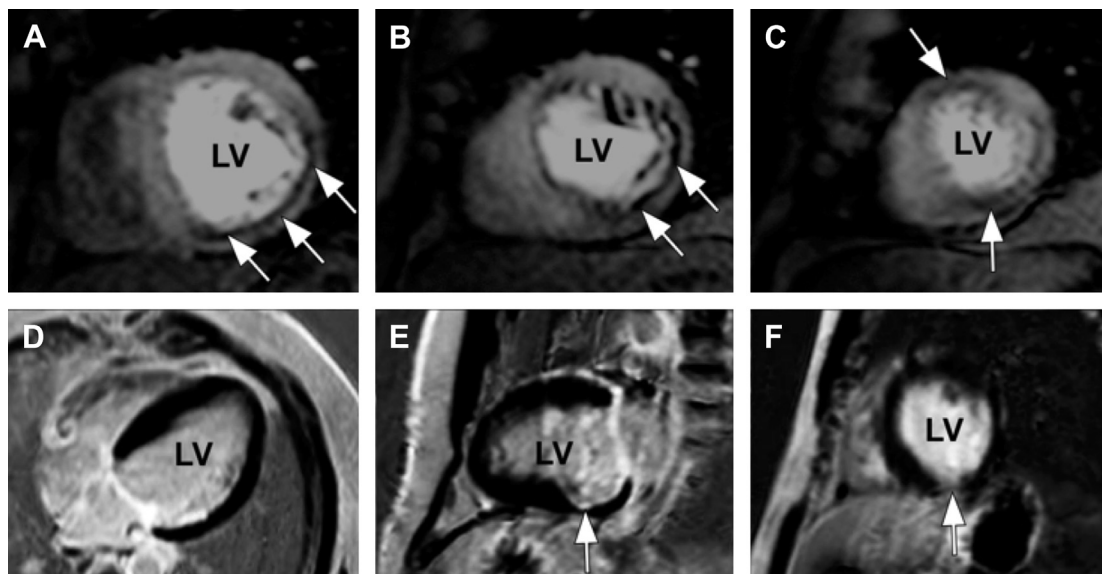


Fig. 1. Stress CMR perfusion examination in a 54-year-old man with exercise-induced chest pain, referred for ischemia assessment. (A-C) Stress first-pass perfusion images acquired during vasodilator pharmacologic stress, demonstrating a large subendocardial perfusion defect within the basal to mid-inferior and lateral LV walls as well as the apical anterior LV segment. (D-F) LGE images showing a small subendocardial myocardial infarction in the inferolateral wall (arrows). The stress perfusion first-pass defect was significantly larger than the areas with documented scar by LGE.

Compared with single photon emission computed tomography (SPECT),⁵ multivendor studies demonstrated noninferior performance of stress perfusion CMR in the presence of at least one-vessel disease and a better performance in multivessel disease.⁶ More recently, the CE-MARC study reported superiority of CMR, even in patients with single-vessel coronary disease.^{4,7} Compared with SPECT, PET offers a better spatial resolution (5–7 mm vs 12–15 mm of SPECT) and the promise not to misdiagnose microvascular or balanced multivessel disease. Also, PET provides absolute quantitative measures of radiotracer concentration, thus facilitating estimation of absolute myocardial perfusion in mL/min per g of myocardial tissue. However, radioisotopes have very a short half-life, requiring on-site production of tracers, which impedes more widespread use. Some other important limitations of nuclear perfusion imaging are the presence of attenuation artifacts, in the anterior wall for female patients with large breasts, and the inferior wall in male patients with large abdominal circumference, use of radiation, and relatively long examination duration.

In this scenario, CMR imaging could have growing importance because it has widespread availability, allows imaging with high temporal and spatial resolution, and does not involve ionizing radiation. However, some shortcomings still prevent CMR from reaching its full potential.

The most important of them is the lack of a dependable quantitative analysis because signal intensities on CMR images do not provide a direct measure of contrast concentration and require careful “calibration” of the contrast concentration estimation in the arterial input. Quantitative analyses are not routinely endorsed by current guidelines, despite their potential clinical utility, because of the lack of clinical studies demonstrating a positive difference in outcomes or even studies confirming a better accuracy compared with nonquantitative visual analysis.^{8,9} In the present review, we aim to gather and appraise pivotal studies related to stress perfusion CMR and present the current state-of-the-art myocardial ischemia assessment by this promising method. The review has a special focus on quantitative analysis of ischemic myocardium.

NORMAL CORONARY FLOW DURING REST AND HYPEREMIA

The established physiologic rationale for stress perfusion imaging is based on the concept of coronary flow reserve.¹⁰ The myocardium extracts virtually all oxygen delivered. Because of the high energy costs for the cardiac cycle, myocardial perfusion depends almost exclusively on coronary blood flow. Coronary flow reserve (Fig. 2) refers to the capacity of the coronary circulation to increase

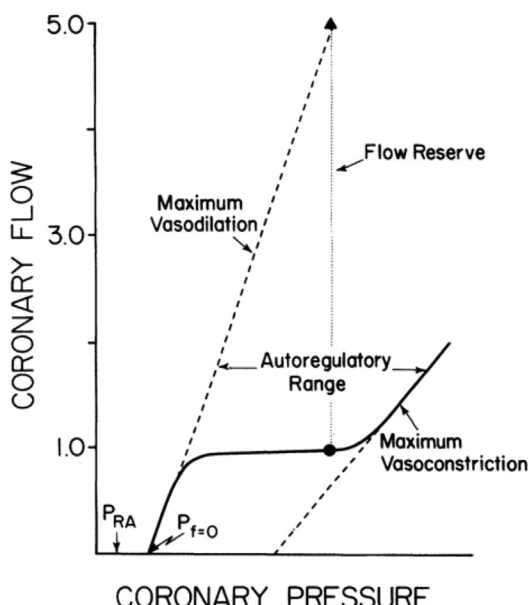


Fig. 2. Association of coronary flow with coronary arterial pressure in the LV. Normal relationship is seen in the solid line. At rest, coronary flow is conserved constant regardless of coronary pressure, between the limits of maximum coronary vasodilation and constriction (dashed lines). The solid circle represents basal conditions; the solid triangle represents flow at the same pressure during maximum vasodilation. Flow reserve is the ratio of flow during vasodilation to that measured before vasodilation, and in this example is 5.0. P_{RA} , right atrial pressure; $P_{f=0}$, back pressure opposing coronary flow. (From Klocke FJ. Measurements of coronary flow reserve: defining pathophysiology versus making decisions about patient care. *Circulation*. 1987;76(6):1183–1189. <https://doi.org/10.1161/01.cir.76.6.1183>; with permission).

the blood flow through the coronary tree until its microcirculation, when in maximum dilation. As for perfusion, it is expressed as the volume of blood flow (eg, in milliliters) through the microcirculation in a unit of myocardial mass (eg, gram), per unit of time (eg, minute). During CMR, coronary artery vasodilation is typically obtained with a pharmacologic vasodilator agent, such as adenosine or dipyridamole, and more recently with regadenoson,^{11,12} an A2A adenosine receptor agonist with fewer side effects than adenosine. In healthy young adults, these drugs increase coronary flow up to 4 times and are particularly effective in minimizing resistance within distal coronary artery bed.

At rest, a coronary epicardial lesion will limit flow only when luminal narrowing reaches 85% or more, whereas with vasodilation this threshold is reduced to approximately 50%.^{13,14} The response of coronary flow to vigorous exercise has the same magnitude as the increase observed during the

vasodilation with an adenosine receptor agonist agent.¹⁵ Presuming that myocardial perfusion can be independently quantified at rest and during maximal vasodilatation, the perfusion reserve can be calculated as the flow rate during hyperemia (maximal vasodilatation) divided by the resting flow. (Sometimes the resting flow in the denominator is normalized by the rate-pressure product to achieve greater independence from the baseline cardiac workload, which can be elevated in hypertension and other pathologies.) In the healthy coronary circulation, the coronary flow reserve and myocardial perfusion reserve agree in magnitude, but the presence of a coronary epicardial obstruction can result in an epicardial reserve inferior to the myocardial perfusion reserve measured downstream of the lesion¹⁶ due to the presence of coronary collaterals. The poststenosis vasodilatory response occurs at the prearteriolar level and depends on individual microvascular function, which, in turn, is determined by clinical factors, such as smoking status, diabetes, hypertension, and other conditions, known to impair microvascular function and induce endothelial dysfunction. Therefore, perfusion of the microcirculation may vary across individuals for a similar epicardial stenosis.

A compromised myocardial perfusion reserve is considered a useful substitute marker for ischemia, although the threshold below which myocardial perfusion reserve should fall to cause clinically relevant ischemia is not well defined. A coronary flow reserve of 2.5:1.0 has frequently been used as a cutoff point, as it results in a significant association with risk factors, presence of CAD, and with clinical outcomes after revascularization.¹⁷ For CMR perfusion imaging with absolute myocardial blood flow (MBF) quantification a similar threshold may be appropriate.

DIAGNOSIS OF CORONARY ARTERY DISEASE

Myocardial Perfusion Imaging

Myocardial perfusion images are acquired for approximately 60 beats to cover a precontrast phase, the first pass of contrast in myocardium after injection, and recirculation of the contrast agent. Total time of acquisition is too long for a single breath-hold, although patients are usually asked to hold their breath for the initial phase of the study and resume breathing when necessary, but without having to take a deep breath, which would result in slice position misregistration. Breathing movement is sufficiently slow to not cause motion artifacts in individual images (acquisition time per image ~120–200 ms), but during postprocessing it is necessary to adjust for respiration-related cardiac motion. However, total

correction for cardiac motion can probably only be solved with 3-dimensional (3D) acquisitions rather than 2D multislice imaging.

A substantial number of single-center^{18–21} and multicenter^{2,3} studies demonstrated favorable sensitivity and specificity of myocardial perfusion imaging with coronary vasodilation for the detection of CAD versus coronary angiography. Stress testing with adenosine yielded better sensitivity for diagnosis of CAD than dipyridamole (0.90, 95% confidence interval [CI]: 0.88–0.92 vs 0.86; 95% CI: 0.80–0.90; $P = .022$) and a trend toward a better specificity (0.81, 95% CI: 0.78–0.84 vs 0.77, 95% CI: 0.71–0.82, $P = .065$). In one multicenter study, Schwitzer and colleagues²² compared the diagnostic accuracy of myocardial perfusion stress by CMR with SPECT for the detection of significant CAD, defined as luminal narrowing $\geq 50\%$ in at least 1 vessel. The investigators demonstrated noninferiority of myocardial perfusion stress CMR (area under the receiver operating characteristic curve [AUC], 0.86 + 0.06 vs 0.75 + 0.09; $P = .12$). Recent meta-analyses^{6,23} confirmed this diagnostic accuracy.

The MR IMPACT II trial ($n = 533$) showed that CMR is a safe alternative to SPECT, revealing greater sensitivity (0.67 vs 0.59, $P = .024$), although lower specificity (0.61 vs 0.72, $P = .038$).⁵ However, in another prospective study ($n = 752$), CE-MARC, Greenwood and colleagues⁴ demonstrated greater sensitivity (86.5% vs 66.5%, $P < .0001$) and negative predictive value (90.5% vs 79.1%, $P < .0001$) of CMR compared with SPECT, whereas specificity (83.4% vs 82.6%, $P = .916$; respectively) and positive predictive value (77.2% vs 71.4%, $P = .061$, respectively) were similar. In addition, stress CMR was superior to SPECT flow limiting CAD across all CAD definitions (Fig. 3). Comparisons with invasive physiologic measures as fractional flow reserve (FFR) also yielded favorable results. Rieber and colleagues²⁴ demonstrated that the calculation of myocardial perfusion reserve index, with a cutoff value of 1.5:1.0 for a semiquantitative perfusion reserve index, allowed the detection of stenosis hemodynamically important, as determined by FFR less than 0.75.

MYOCARDIAL PERFUSION QUANTIFICATION

Semiquantitative Analysis

Semiquantitative techniques assess the signal intensity versus time curves across myocardial segments by determining simple curve properties, rather than estimating MBF.⁹ Briefly, a segmentation model of 17 segments, as recommended by the American Heart Association,²⁵ divides the left

ventricle (LV) in regions to be analyzed in parallel with wall motion and LGE. Myocardial segments are defined on short-axis views of the heart (and possibly 1 long-axis view for apical cap) by contouring the LV along the endocardial and epicardial borders, defining a reference point like the anterior LV-right ventricle junction, and subdividing the LV wall into 6 segments at the basal and mid-level, and 4 segments at the apical level. This form of segmentation of the LV allows tracking of the same portions of the LV wall, compensates for respiratory movements, and excludes epicardial fat and signal from the blood pool as potential sources of error. Images acquired during ectopic heartbeats are excluded. The rate of increase of the signal intensity during the first pass ("upslope" of signal-intensity curve) has been identified as useful parameter for a semi-quantitative analyses and shown to yield good diagnostic accuracy.^{3,20,21,26} Frequently evaluated parameters by postprocessing packages include maximal upslope of the myocardial signal intensity, AUC from start of contrast enhancement to first-pass peak in the blood pool,⁹ and time to peak signal intensity (from start of contrast enhancement).

Estimating the spatial extent of ischemia provides important diagnostic and prognostic information. A recent prospective study with 1024 consecutive patients referred to stress perfusion CMR suggests that simple quantification of the number of ischemic segments has a prognostic value and helps identify patients at risk.²⁷ Based on the 16-segment model (17-segment model excluding the apical cap), the investigators demonstrated that patients with ≥ 1.5 ischemic segments presented a worse prognosis, owing to more frequent cardiac death, nonfatal myocardial infarction, and myocardial revascularization within 90 days of the examination. The mean follow-up time of the study was 2.5 years. In the 17-segment model, ischemia in 2 or more segments corresponds to approximately a 12.0% ischemic burden mirroring nuclear medicine studies in which an ischemic load greater than 10.0% to 12.5% should be used to indicate coronary revascularization because myocardium would be at risk.

Full Quantification of Myocardial Perfusion

Fully automated quantitative analyses are still not established in clinical practice but have evolved and may help discriminate diagnosis in particular cases such as multivessel coronary disease, microvascular dysfunction, or suspicion of inadequate vasodilator response. Quantitative

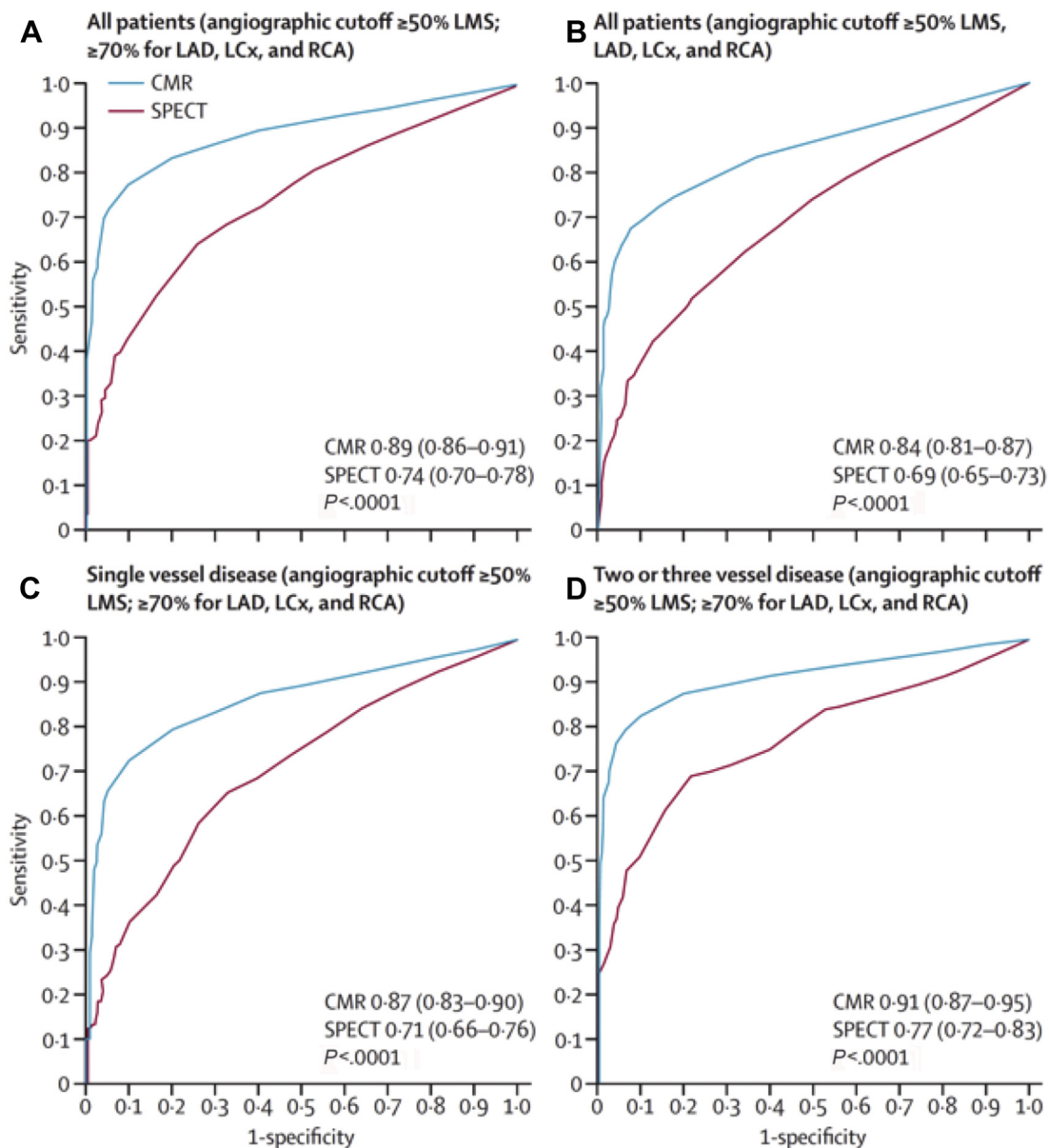


Fig. 3. Receiver operating characteristic curves comparing stress CMR (blue line) and SPECT (pink line) for detecting flow limiting CAD according to coronary heart disease definition (A) all patients with angiographic cutoff $\geq 50\%$ for LMS or $\geq 70\%$ for LAD, LCx and RCA; (B) all patients with angiographic cutoff $\geq 50\%$ for LMS, LAD, LCx and RCA; (C) single vessel disease with angiographic cutoff $\geq 50\%$ for LMS or $\geq 70\%$ for LAD, LCx and RCA and (D) two or three vessel disease with angiographic cutoff $\geq 50\%$ for LMS or $\geq 70\%$ for LAD, LCx and RCA. LAD, left anterior descending; LCx, left circumflex; LMS, left main stenosis; RCA, right coronary artery. (Reprinted with permission from Elsevier [Greenwood JP, Maredia N, Younger JF, et al. Cardiovascular magnetic resonance and single-photo emission computed tomography for diagnosis of coronary heart disease (CE-MARC): a prospective trial. Lancet 2012;379(9814):453–60].)

CMR has been validated against microspheres in experimental models,²⁸ coronary sinus flow,²⁹ and PET in healthy volunteers.³⁰

In patients undergoing coronary angiography, Morton and colleagues³¹ applied a double bolus injection and Fermi deconvolution analysis to

fully quantitative stress perfusion by CMR and compare it with ^{13}N -ammonia PET, the current noninvasive reference standard. They demonstrated that myocardial perfusion reserve is highly correlated between the 2 methods ($r = 0.75$, $P < .0001$). When analyzing coronary

territories with the lowest reserve scores, correlation remained significant ($r = 0.79, P < .0001$). However, absolute perfusion values, at rest and during stress, had only a modest association ($r = 0.32, P < .002$ and $r = 0.37, P < .0001$, respectively). These data may be explained by different properties of the tracers and model assumptions, but the relative stress/rest ratios are less affected by absolute disparities. The same study established cut-off values for MBF reserve that predicted significant coronary disease determined by angiography: ≤ 1.44 for PET and ≤ 1.45 for CMR (with 82% sensitivity and 87% specificity; and 82% sensitivity and 81% specificity, respectively). Different approaches have been proposed for MBF quantification, are frequently applied and appear to have similar diagnostic performance.³² They are Fermi model, uptake model, 1-compartment model, model-independent deconvolution methods, and 2 model-independent methods.

Gadolinium Enhancement and Myocardial Blood Flow

These fully quantitative methods derive estimates of MBF from signal intensity versus time curves of myocardial contrast enhancement. Yet, signal intensity is only approximately proportional to gadolinium concentration in T1-weighted images and at higher concentrations this relation becomes nonlinear, giving rise to what is often referred to as signal saturation. Signal saturation in particular affects the signal intensity in the blood pool, where contrast concentrations are highest during the first pass compared with myocardium. Several options are available to avoid or minimize this problem: the contrast dose and delivery must be chosen to minimize saturation effects and doses are often lower than those applied in routine practice for visual interpretation of studies. A dual bolus of contrast with a dosage (or dilution) ratio of approximately 1:10 may help minimize saturation effects in the arterial input during the first pass of the lower-dosage bolus. The second larger bolus is used for measuring myocardial contrast enhancement, although it should be pointed out that saturation may still affect the vascular component of the signal in the myocardium, but there are no visual cues of saturation like in the case of the arterial input. For a quantitative analysis, the arterial input measured with the small bolus is scaled up to the dosage used for the measurement of the myocardial enhancement, and aligned with the start of blood pool enhancement from the second bolus. As can be surmised from the signal intensity curves measured with a dual-bolus technique, postprocessing requires selecting portions of signal-intensity curves for arterial input and

myocardial enhancement, respectively, matching them up along the time axis, all requiring user input (Fig. 4).^{28,33} A so-called dual-sequence approach may be an alternative to the dual bolus because it is based on the combined measurement of the blood pool input function and myocardial signals with different T1 weighting. For the arterial input images, one acquires low-resolution images within less than ~ 40 ms with a T1 weighting that is less sensitive to T1 changes but offers a wider linear range (for the relationship between signal intensity and $R_1 = 1/T_1$), followed by myocardial images with a stronger T1 weighting of the signal intensity, but smaller linear range. The dual-sequence approach avoids variation between bolus injections,³⁴ and ensures almost perfect temporal alignment for the signal intensity curves depicting contrast enhancement in the arterial input and myocardial segments.

Two approaches have been applied for the quantification of MBF from regional signal intensity curves: one is based on a tracer-kinetic model for the blood-tissue exchange (BTEX)^{35,36} of contrast, representing the vascular and interstitial compartments as functional spaces between which contrast is exchanged via a (capillary) barrier, after contrast enters the tissue through its arterial input. This BTEX type of model was first applied for quantification of myocardial perfusion with an intravascular contrast agent by Kroll and colleagues³⁵ and later used also for studies with extravascular agents. It required careful adjustment of some fixed parameters of the model, as one can generally only leave blood flow and 1 volume parameter as variable fitting parameters to ensure reproducible results. (Alternatively, one can use an intravascular contrast agent, which allows simplification of the model.) A second approach for quantification is based on the central volume theorem of Meier and Zierler,³⁷ which states that the amplitude of the myocardial impulse response equals blood flow. It is illustrated in Fig. 5. Furthermore, the myocardial impulse response, when convolved with a measured arterial input, predicts the myocardial contrast enhancement. To be of practical value, this relationship between the myocardial impulse response and myocardial enhancement has to be inverted to estimate blood flow: the impulse response is estimated by deconvolving the measured myocardial contrast enhancement curve, with the measured arterial contrast enhancement curve. Deconvolution falls into a category of mathematical problems that are termed "ill-posed," as there is no mathematically unique solution, and one has to effectively apply constraints based on physiologic or empirical

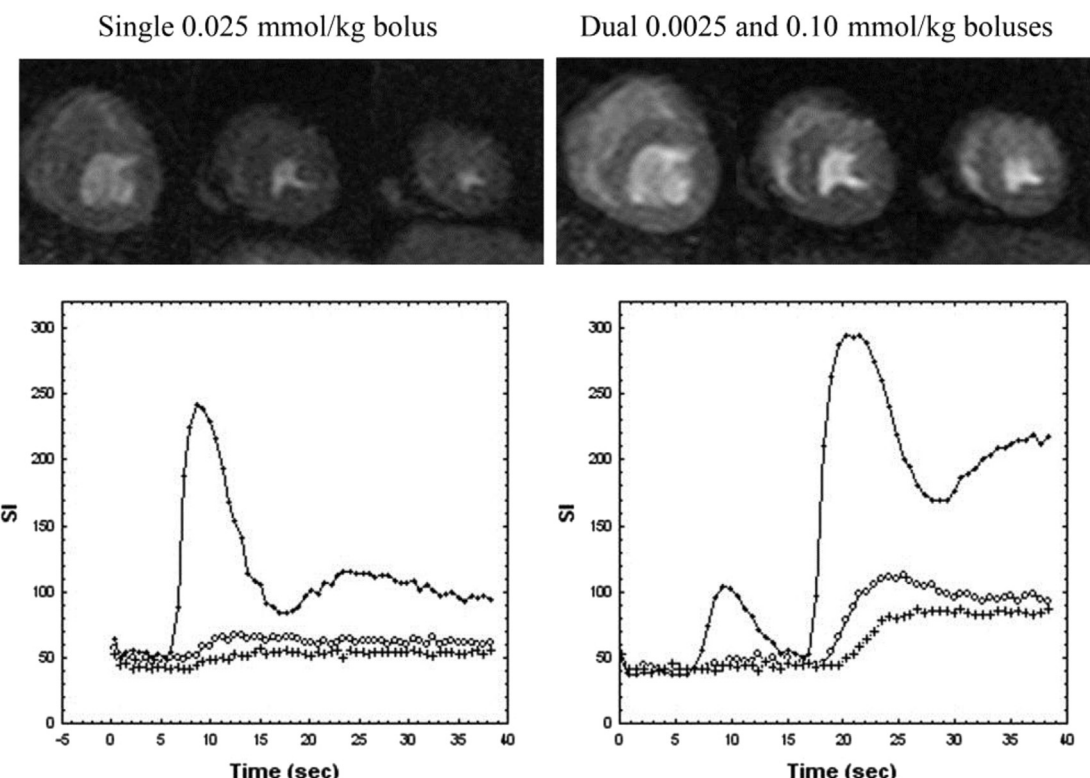


Fig. 4. Compared with single-bolus low-contrast injection (upper and lower left panels), high-contrast dual-bolus injection (upper and lower right panels), has less variability and better image quality. SI, signal intensity. (From Christian TF, Aletras AH, Arai AE. Estimation of absolute myocardial blood flow during first-pass MR perfusion imaging using a dual-bolus injection technique: Comparison to single-bolus injection method. *J Magn Reson Imaging*. 2008;27(6):1271–1277; with permission).

insights to recover a solution that represents a good “physiologic” approximation.³⁸ One approach is to constrain the impulse response to a certain class of shapes, based on observations from simulations with tracer-kinetic problems. A Fermi function has proven to be a reasonable approximation for the tissue impulse response,³⁹ at least during first pass of the contrast agent, and used as a parametrized representation of the impulse response for deconvolution of the measured myocardial contrast enhancement.⁴⁰ An advantage of the “deconvolution” approach is that it obviates the need a model of the BTEX, that may include parameters with poor sensitivity to the measurement conditions, and therefore may require some user adjustment. For further details the reader is referred to earlier reviews on blood flow quantification by CMR.^{40,41}

High Spatial Resolution

A variety of recent techniques have provided a more than 10-fold reduction in image acquisition time from undersampling of the image data by taking advantage of spatial, temporal, or spatio-

temporal redundancy in the image data.^{42–44} Spatial redundancy follows from use of parallel receive coils/channels, and gave rise to parallel-imaging acceleration techniques. Temporal redundancy is due to the serial acquisition of images for a single time point in cardiac cycle, and because contrast enhancement proceeds at a slower rate than the image acquisition rate. These forms of data-redundancy in a “conventional” perfusion scan (ie, without use of undersampling) imply that undersampling in both the spatial and time domains ($k\text{-}t$) can be performed to reduce the image acquisition time within bounds deemed acceptable for signal-to-noise, image quality, artifact absence, and so forth. Various $k\text{-}t$ undersampling/acceleration techniques have been used for myocardial perfusion CMR, such as TSENSE,^{45,46} $k\text{-}t$ BLAST,⁴⁷ and more recently $k\text{-}t$ principal component analysis (PCA).^{48,49} Other, arguably more esoteric methods relate to the highly constrained back-projection reconstruction (HYPR),⁵⁰ in which k -space data are obtained by undersampled radial projections, possibly combined with an overall rotation of the sampling pattern during the course of dynamic imaging.

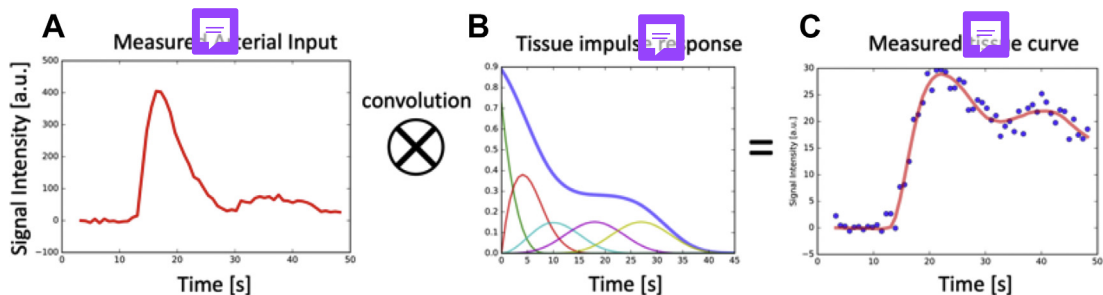


Fig. 5. The central volume principle of Meier and Zierler³⁷ states that the convolution of arterial input, shown in (A), with the myocardial impulse response in (B), predicts the myocardial response that would be observed, shown as solid red line in (C). Meier and Zierler³⁷ deduced from first principles that the amplitude of the impulse response equals MBF. In this example from a rest perfusion study, the arterial input and the myocardial contrast enhancement (circles in C) were extracted from CMR perfusion images. To estimate the impulse response from these measured curves, one must invert the relationship depicted in the figure and apply a *deconvolution* operation. Convolution can be thought of as a complex form of multiplication. Deconvolution would then be akin to division and is susceptible to producing spurious results from noise in the data. For a stable deconvolution, we required the impulse response to be smooth and monotonically decaying; contrast can only leave a region after an initial impulse input. Smoothness was enforced by representing the impulse response as a sum of smooth "basis" splines, shown as individual components under the blue curve in (B). MBF in this example was estimated to be 0.9 mL/min per g; the initial amplitude of the impulse response.

Missing data due to undersampling is restored from neighboring time frames.^{50,51} This technique also presents a greater signal-to-noise ratio adjusted for pixel size.⁵² The gains from imaging acceleration have been put to use to allow an in-plane spatial resolution of below 1.5 to 2.0 mm and still acquire 3 to 4 images per heartbeat, whereas traditional studies achieved an in-plane resolution of 2.5 to 3.0 mm for a similar number of slices per heartbeat.^{4,5,22}

In CMR perfusion imaging, higher spatial resolution significantly reduces dark-rim artifacts because they are proportional to voxel size.⁵³ Application of *k-t* techniques in 3.0 T may reach up to eightfold acceleration and a resolution of 1.1 mm. This combination improved diagnostic performance of the method in CAD-suspected patients undergoing angiography (AUC, 0.93 vs 0.83; $P < .001$), which can be attributed to a better detection of subendocardial ischemia.⁵⁴ Quantitative analyses based on high-resolution perfusion stress imaging seems to be feasible and may even allow assessment of transmural gradients. However, temporal filtering effects inherent to *k-t* acceleration techniques may introduce a bias of underestimating blood flows and further optimization may still be needed to define the clinically acceptable limits for imaging acceleration.⁵⁵

Three-Dimensional Whole-Heart Coverage

Faster image acquisition also paved the way for the development of whole-heart 3D myocardial perfusion CMR imaging. Three-dimensional perfusion CMR conceivably addresses an important limitation

of the multislice 2D imaging, which is the lack of complete myocardial coverage (in 2D, only 3–4 noncontiguous slices are obtained). Also, in 2D CMR sequences, slices correspond to different phases of the cardiac, whereas in 3D, acquisition is made in a diastolic phase and can be matched with other data obtained, for instance, of LGE.⁵⁵ A drawback of 3D perfusion imaging is that one can use only a relatively short fraction of the cardiac cycle for the acquisition of image data in order to minimize artifacts from cardiac motion. With 2D perfusion imaging, the acquisition of image data for each slice is self-contained, and avoidance of motion-induced artifacts or blurring involves minimizing this acquisition time per slice rather than the total acquisition time during each cardiac cycle.

Visually interpreted 3D-CMR perfusion examinations have achieved promising results, although superiority of 3D compared with 2D perfusion imaging remains to be shown in head-to-head comparisons. Manka and colleagues⁵⁶ assessed 146 patients at suspicion for CAD with a *k-t* imaging acceleration technique achieving 2.3-mm spatial resolution, and found sensitivity of 92%, specificity of 74%, and accuracy of 83% compared with quantitative coronary angiography $\geq 50\%$. At 3.0 T, diagnosis accuracy reaches 91% (sensitivity of 90% and specificity of 90%) when the standard comparison is a physiology method such as FFR by angiography.⁵⁷

As for quantitative analyses, multicenter data demonstrate accuracy of 3D CMR perfusion imaging and accurate quantification of the ischemic volume relative to the entire myocardium.^{56,58–60} Newly developed protocols have been released

and promising results published. Fully 3D quantitative evaluations of MBF would eliminate the necessity to identify a "normally" perfused region of myocardium as reference, and could match up with the standard quantitative method PET but with the advantage of widespread availability, better spatial resolution, and absence of harmful radiation. Notwithstanding, some of the drawbacks related to the method must be addressed, such as the requirement for accurate arterial input sampling. A dual-sequence/dual-contrast using $k\text{-}t$ PCA for spatially and temporally undersampled data yielded 3D perfusion images with higher signal-to-noise ratio (at contrast doses of 0.1 mmol/kg, and compared with 2D perfusion imaging), and addressed the issue of nonlinear (in relation to contrast concentration) contrast enhancement.⁶¹ Acquisition of data for $k\text{-}t$ PCA 3D perfusion imaging may take place either in diastole or systole,⁶² but with a possible preference for systole because the LV wall is thicker, thereby facilitating an analysis of subendocardial perfusion. Also, during systole, dark-rim artifacts, which tend to have a constant width independent of cardiac phase, tend to be less of a nuisance than for diastolic images with a thinner LV wall. Other shortcomings of 3D fully quantitative analyses still need further research, such as a lack of standardized contrast-dosing, imaging acquisition and postprocessing protocols. More importantly, large clinical trials need to validate the current findings.

Microvascular Perfusion

Microvascular disease may appear as a subendocardial concentric perfusion defect. As it may not respect coronary territories its diagnosis may be difficult. It frequently coincides with the presence of LV hypertrophy and in individuals with diseases that lead to capillary rarefaction or dysfunction of the microcirculation, such as diabetes and hypertension. The appearance of a diffuse subendocardial perfusion defect may also take place in the presence of balanced multivessel coronary disease and a differential diagnosis may be challenging. In addition, although coronary angiography may differentiate microvascular disease and multivessel epicardial (macrovascular) disease, it may lead to inappropriate exclusion of microvascular disease when it is in fact present if accurate tools to rule out the diagnosis are not applied during angiography.^{63–66}

Assessment of Wall Motion Segmental Contractility

Exercise has already been used in CMR to induce ischemia,⁶⁷ but the logistics to reach a sufficient

level of exercise is difficult to impossible within the confines of a magnet bore and pharmacologic stress remains the method of choice for clinical CMR studies. As the heterogeneity of the flow does not lead directly to ischemic abnormalities of wall motion except in cases of more severe perfusion reduction, it is not surprising that the assessment of wall motion during vasodilator stress results in a lower sensitivity⁶⁸ and higher specificity for the detection of coronary disease than the use of inotropic drugs. Therefore, stress-related contractility assessment should be preferably carried out with inotropes.

Nagel and colleagues⁶⁹ compared the segmental abnormalities of the LV wall induced by ischemia during dobutamine infusion by CMR with stress echocardiography in 208 consecutive patients with suspected CAD before cardiac catheterization. In this study, dobutamine CMR provided better sensitivity (89% vs 74%) and specificity (86% vs 70%) than stress echocardiography with dobutamine to detect coronary artery stenosis greater than 50%. Likewise, Hundley and colleagues,⁷⁰ using dobutamine in 163 patients with unfavorable echocardiographic windows, demonstrated sensitivity and specificity of 83% in the detection of coronary stenosis greater than 50% per coronary angiography. Various studies of CMR using dobutamine to induce of ischemia suggest that the presence of segmental contractile dysfunction in only 1 segment (6% of ischemic load) is already a predictor of worse outcome.^{71,72} Any difference between the number of segments with reduced perfusion and the number of segments with wall motion abnormalities could be explained by the sequence of events in the ischemic cascade. As hypoperfusion precedes contraction abnormalities, it is possible that the extent of hypoperfusion exceeds the hypokinetic segments.

Myocardial Viability

Assessment of contractile reserve, as in stress echocardiography, was the first approach to assessing myocardial viability by CMR, but the technique has evolved considerably with the introduction of LGE images.⁷³ Viability can be estimated by wall thickness ratio (rest/stress), contractile reserve, and LGE currently considered gold-standard method for viability.^{74,75}

Myocardial Contractile Reserve and Relative Wall Thickness

In line with echocardiographic data,⁷¹ the presence of thinned myocardium can indicate lack of viability. Baer and colleagues⁷² demonstrated

that a diastolic wall thickness of 5.5 mm could be used to delimit myocardial segments with preserved metabolic function from those without, as evaluated by FDG PET. In a later study, the same group demonstrated that was almost never a recovery of regional function when the thickness of diastolic wall was less than 5.5 mm⁷⁶; however, the reverse was not always true, that is, functional recovery did not occur universally in regions with wall thickness greater than 5.5 mm. Thus, the evaluation of diastolic wall thickness, although sensitive, offers poor specificity for predicting functional recovery.

Thickening of the ventricular wall of 2 mm during low-dose dobutamine greatly improves the specificity of technique. In the study by Baer and colleagues,⁷⁶ dobutamine increased specificity to 92% with sensitivity remaining at 86% to predict post-revascularization functional recovery. A consistent finding in dobutamine stress, however, is the high specificity of the technique, similar to the stress echocardiogram.⁷⁷ To achieve higher observer-independence techniques, such as tissue “tagging” and feature tracking for the analysis of myocardial deformation (“strain”) offer the potential to further improve on the reported results, although the additional postprocessing required by these techniques has been a persistent deterrent to their clinical application.

Late Gadolinium Enhancement

Excellent tissue characterization is one of the main advantages of CMR and the exploitation of this through the use of T1-weighted contrast images to define infarcted and irreversibly damaged myocardium has been one of the most significant advances in CMR.⁷³ Although the exact reasons for the hypersignal in replacement (or interstitial) fibrosis continue to be a subject of intense scrutiny, the likely mechanism is a combination of arrival and output kinetics of the gadolinium within the myocardium and different volumes of distribution of gadolinium in viable cells and nonviable regions. The injected extracellular gadolinium contrast agent distributes within the entire tissue volume after myocardial infarction, whereas in normal myocardium, gadolinium is excluded from the intracellular space, that is, from approximately two-thirds of the tissue volume.

In acute myocardial ischemia the integrity of the membrane of the sarcolemma is lost, effectively a marker of cell death, allowing gadolinium to get into cardiomyocytes and resulting in signal hyperintensity. In chronic disease, the tissue transforms into a dense collagen matrix with a greatly expanded interstitial space accessible to

gadolinium contrast. Although some animal studies have demonstrated that the size and transmural depth of the infarction may be slightly overestimated (9%–12%) in the immediate postinfarction phase, these indicators are stable and reflect the actual extension of the scar after 1 week.

Late Gadolinium Enhancement in Clinical Practice

Experimental and clinical studies indicate that the extent of LGE is reproducible and closely correlates with the size of the myocardial necrosis or scar of infarction as determined by *in vitro* and *in vivo* methods established.^{78–80} Subendocardial LGE is highly specific for the detection of myocardial infarction.⁷⁸ In addition, the detection of myocardial infarction is associated with a significantly increased risk of death subsequent to adverse cardiac events, adding incremental prognostic information to the evaluation of ventricular function.^{81,82} Finally, the extent of myocardial LGE is emerging as a tool to determine the response to new medical and interventional therapies. The probability of functional recovery by segment is inversely related to the transmural extension of the infarct.⁷⁵ Zero percent to 25% transmural extension is associated with 82% probability of contractile function recovery, a 26% to 50% transmural extension, with 45% probability of recovery, and among segments with 51% to 75% transmural extension only 7% recovered. None of the segments presented recovery when the transmural extent of LGE was 75% or larger. Subsequent studies by other groups corroborated these results.^{83–85} In addition to the response to revascularization, the extent of viable myocardium in ischemic cardiomyopathy also appears to be a predictor of response to beta-blockade⁸⁶ and myocardial scar may be useful in the selection of patients who will benefit from resynchronization therapy.⁸⁷

Clinical Prognosis Assessment

Coelho-Filho and colleagues⁸⁸ demonstrated in a relatively large number of women and men, that there were no significant differences between men and women regarding the diagnosis of CAD or for risk stratification of major adverse cardiovascular events using CMR stress perfusion imaging. But the method can shed light on the pathophysiology of chest pain with normal epicardial coronary arteries (“syndrome X”), a clinically not uncommon distressing condition in postmenopausal women. Quantitative myocardial perfusion CMR⁸⁹ has been validated against invasive

measurements of coronary flow reserve in patients with microvascular dysfunction; it was found to provide excellent correlation with the catheter-based measurements. Panting and colleagues⁶⁵ identified myocardial subendocardial hypoperfusion during adenosine infusion in this set of patients (X syndrome), and Doyle and colleagues⁹⁰ reported reduction in coronary flow reserve in similar patients. Coronary flow reserve is also reduced in hypertension, myocardial hypertrophy,^{91,92} and in some cardiomyopathies.⁹³

Acute Chest Pain

Stress perfusion CMR can provide prognostic information in various clinical settings.^{94–96} In the acute chest pain scenario, Ingkanisorn and colleagues⁹⁴ have shown that adenosine stress CMR may determine the prognosis in patients with inconclusive electrocardiogram for CAD and negative biomarkers for acute coronary syndrome. In such patients, a negative perfusion stress CMR virtually excluded CAD or unfavorable clinical outcomes: no patient with normal examination had an adverse cardiac event. In a population with chest pain presenting to the emergency department, perfusion stress CMR was shown to have a sensitivity of 100% and a 93% specificity in the prediction of subsequent myocardial infarction or detection of coronary stenosis during 1 year of follow-up.⁹⁵

Chronic Chest Pain

Results are similar for patients with suspected CAD. In a cohort of 513 patients, Jahnke and colleagues⁹⁷ examined the value of adenosine stress CMR perfusion and dobutamine stress CMR to help predict cardiac death and nonfatal myocardial infarction. At 3 years of follow-up, event-free survival reached 99.2% for patients with normal CMR and 83.5% for those with an abnormal perfusion. Abnormal CMR yielded a probability of death or nonfatal infarction beyond estimated risk from the presence of clinical risk factors (likelihood ratio, $\chi^2 = 16.0\text{--}34.3$, $P = .001$). In this study, stress CMR, either by perfusion or by wall motility, contributed with incremental value regarding traditional factors such as age, sex, smoking and diabetes, although the combination of both techniques did not increase stratification power. A normal perfusion was associated with an event rate extremely low, 0.7% at 2 years, 2.3% at 3 years, and an abnormal perfusion study with corresponding rates of 6.2%, 12.2%, and 16.3%. In the multivariate analysis, adjusting for other risks, the detection of an abnormality of perfusion was associated with a 10-fold increase in risk of

cardiovascular events (death or myocardial infarction). In another study of 218 patients with negative perfusion studies followed for more than 2 years, there were no deaths or infarction, percutaneous coronary intervention or coronary revascularization surgery.⁹⁸

SUMMARY

CMR provides excellent temporal and spatial resolution without the limitations associated with unfavorable echocardiographic windows, and low temporal and spatial resolution in nuclear medicine studies, nor does it involve ionizing radiation. Myocardial perfusion by CMR can be integrated with a spatially registered interrogation of regional function (wall thickening, segmental contractility, and myocardial deformation image), edema, fibrosis, and viability. These simultaneous faculties are not present in other imaging modalities. Quantitative analysis of myocardial perfusion is an evolving tool for stress perfusion CMR and may be incorporated into clinical practice within the next few years. Larger clinical studies are expected to pave the way for wider adoption. Although every other cardiac imaging modality may offer one equivalent or possibly superior match for assessing stress perfusion or function, fibrosis, or viability, the key to the success of CMR may lie in the power of an integrated cardiac examination in which each of these components provides an incremental benefit for diagnosis and prognosis. In that context, stress perfusion CMR will undoubtedly play a pivotal role for improving the diagnosis of myocardial ischemia and add to the already outstanding capabilities of CMR for assessing ventricular function and myocardial viability.

REFERENCES

1. Coelho-Filho OR, Rickers C, Kwong RY, et al. MR myocardial perfusion imaging. *Radiology* 2013; 266(3):701–15.
2. Wolff SD, Schwitter J, Couliden R, et al. Myocardial first-pass perfusion magnetic resonance imaging: a multicenter dose-ranging study. *Circulation* 2004; 110(6):732–7.
3. Giang TH, Nanz D, Couliden R, et al. Detection of coronary artery disease by magnetic resonance myocardial perfusion imaging with various contrast medium doses: first European multi-centre experience. *Eur Heart J* 2004;25(18):1657–65.
4. Greenwood JP, Maredia N, Younger JF, et al. Cardiovascular magnetic resonance and single-photon emission computed tomography for diagnosis of

- coronary heart disease (CE-MARC): a prospective trial. *Lancet* 2012;379(9814):453–60.
5. Schwitser J, Wacker CM, Wilke N, et al. MR-IMPACT II: Magnetic Resonance Imaging for Myocardial Perfusion Assessment in Coronary artery disease Trial: perfusion-cardiac magnetic resonance vs. single-photon emission computed tomography for the detection of coronary artery disease: a comparative multicentre, multivendor trial. *Eur Heart J* 2013; 34(10):775–81.
 6. Hamon M, Fau G, Nee G, et al. Meta-analysis of the diagnostic performance of stress perfusion cardiovascular magnetic resonance for detection of coronary artery disease. *J Cardiovasc Magn Reson* 2010;12(1):29.
 7. Greenwood JP, Motwani M, Maredia N, et al. Comparison of cardiovascular magnetic resonance and single-photon emission computed tomography in women with suspected coronary artery disease from the Clinical Evaluation of Magnetic Resonance Imaging in Coronary Heart Disease (CE-MARC) Trial. *Circulation* 2014;129(10):1129–38.
 8. Puntmann VO, Valbuena S, Hinojar R, et al. Society for Cardiovascular Magnetic Resonance (SCMR) expert consensus for CMR imaging endpoints in clinical research: part I - analytical validation and clinical qualification. *J Cardiovasc Magn Reson* 2018;20(1):67.
 9. Schulz-Menger J, Bluemke DA, Bremerich J, et al. Standardized image interpretation and post processing in cardiovascular magnetic resonance: Society for Cardiovascular Magnetic Resonance (SCMR) board of trustees task force on standardized post processing. *J Cardiovasc Magn Reson* 2013;15:35.
 10. Klocke FJ. Measurements of coronary flow reserve: defining pathophysiology versus making decisions about patient care. *Circulation* 1987; 76(6):1183–9.
 11. Farzaneh-Far A, Shaw LK, Dunning A, et al. Comparison of the prognostic value of regadenoson and adenosine myocardial perfusion imaging. *J Nucl Cardiol* 2015;22(4):600–7.
 12. Iqbal FM, Hage FG, Ahmed A, et al. Comparison of the prognostic value of normal regadenoson with normal adenosine myocardial perfusion imaging with propensity score matching. *JACC Cardiovasc Imaging* 2012;5(10):1014–21.
 13. Gould KL, Kirkeeide RL, Buchi M. Coronary flow reserve as a physiologic measure of stenosis severity. *J Am Coll Cardiol* 1990;15(2):459–74.
 14. Gould KL, Lipscomb K. Effects of coronary stenoses on coronary flow reserve and resistance. *Am J Cardiol* 1974;34(1):48–55.
 15. Duncker DJ, Bache RJ. Regulation of coronary blood flow during exercise. *Physiol Rev* 2008; 88(3):1009–86.
 16. Geldof MJ, Schalij MJ, Manger Cats V, et al. Comparison between regional myocardial perfusion reserve and coronary flow reserve in the canine heart. *Eur Heart J* 1995;16(12):1860–71.
 17. Serruys PW, di Mario C, Piek J, et al. Prognostic value of intracoronary flow velocity and diameter stenosis in assessing the short- and long-term outcomes of coronary balloon angioplasty: the DEBATE Study (Doppler Endpoints Balloon Angioplasty Trial Europe). *Circulation* 1997;96(10):3369–77.
 18. Panting JR, Gatehouse PD, Yang GZ, et al. Echo-planar magnetic resonance myocardial perfusion imaging: parametric map analysis and comparison with thallium SPECT. *J Magn Reson Imaging* 2001; 13(2):192–200.
 19. Klem I, Heitner JF, Shah DJ, et al. Improved detection of coronary artery disease by stress perfusion cardiovascular magnetic resonance with the use of delayed enhancement infarction imaging. *J Am Coll Cardiol* 2006;47(8):1630–8.
 20. Schwitser J, Nanz D, Kneifel S, et al. Assessment of myocardial perfusion in coronary artery disease by magnetic resonance: a comparison with positron emission tomography and coronary angiography. *Circulation* 2001;103(18):2230–5.
 21. Al-Saadi N, Nagel E, Gross M, et al. Noninvasive detection of myocardial ischemia from perfusion reserve based on cardiovascular magnetic resonance. *Circulation* 2000;101(12):1379–83.
 22. Schwitser J, Wacker CM, van Rossum AC, et al. MR-IMPACT: comparison of perfusion-cardiac magnetic resonance with single-photon emission computed tomography for the detection of coronary artery disease in a multicentre, multivendor, randomized trial. *Eur Heart J* 2008;29(4):480–9.
 23. Nandalur KR, Dwamena BA, Choudhri AF, et al. Diagnostic performance of stress cardiac magnetic resonance imaging in the detection of coronary artery disease: a meta-analysis. *J Am Coll Cardiol* 2007;50(14):1343–53.
 24. Rieber J, Jung P, Schiele TM, et al. Safety of FFR-based treatment strategies: the Munich experience. *Z Kardiol* 2002;91(Suppl 3):115–9.
 25. Cerqueira MD, Weissman NJ, Dilsizian V, et al. Standardized myocardial segmentation and nomenclature for tomographic imaging of the heart. A statement for healthcare professionals from the Cardiac Imaging Committee of the Council on Clinical Cardiology of the American Heart Association. *Circulation* 2002;105(4):539–42.
 26. Nagel E, Klein C, Paetsch I, et al. Magnetic resonance perfusion measurements for the noninvasive detection of coronary artery disease. *Circulation* 2003;108(4):432–7.
 27. Vincenti G, Masci PG, Monney P, et al. Stress perfusion CMR in patients with known and suspected CAD: prognostic value and optimal ischemic

- threshold for revascularization. *JACC Cardiovasc Imaging* 2017;10(5):526–37.
- 28. Christian TF, Rettmann DW, Aletras AH, et al. Absolute myocardial perfusion in canines measured by using dual-bolus first-pass MR imaging. *Radiology* 2004;232(3):677–84.
 - 29. Ichihara T, Ishida M, Kitagawa K, et al. Quantitative analysis of first-pass contrast-enhanced myocardial perfusion MRI using a Patlak plot method and blood saturation correction. *Magn Reson Med* 2009;62(2):373–83.
 - 30. Fritz-Hansen T, Hove JD, Kofoed KF, et al. Quantification of MRI measured myocardial perfusion reserve in healthy humans: a comparison with positron emission tomography. *J Magn Reson Imaging* 2008;27(4):818–24.
 - 31. Morton G, Chiribiri A, Ishida M, et al. Quantification of absolute myocardial perfusion in patients with coronary artery disease: comparison between cardiovascular magnetic resonance and positron emission tomography. *J Am Coll Cardiol* 2012;60(16):1546–55.
 - 32. Biglands JD, Magee DR, Sourbron SP, et al. Comparison of the diagnostic performance of four quantitative myocardial perfusion estimation methods used in cardiac MR imaging: CE-MARC Substudy. *Radiology* 2015;275(2):393–402.
 - 33. Christian TF, Aletras AH, Arai AE. Estimation of absolute myocardial blood flow during first-pass MR perfusion imaging using a dual-bolus injection technique: comparison to single-bolus injection method. *J Magn Reson Imaging* 2008;27(6):1271–7.
 - 34. Kellman P, Hansen MS, Nielles-Valdespin S, et al. Myocardial perfusion cardiovascular magnetic resonance: optimized dual sequence and reconstruction for quantification. *J Cardiovasc Magn Reson* 2017;19(1):43.
 - 35. Kroll K, Wilke N, Jerosch-Herold M, et al. Modeling regional myocardial flows from residue functions of an intravascular indicator. *Am J Physiol* 1996;271(4 Pt 2):H1643–55.
 - 36. Jerosch-Herold M, Wilke N, Wang Y, et al. Direct comparison of an intravascular and an extracellular contrast agent for quantification of myocardial perfusion. Cardiac MRI Group. *Int J Card Imaging* 1999;15(6):453–64.
 - 37. Meier P, Zierler KL. On the theory of the indicator-dilution method for measurement of blood flow and volume. *J Appl Physiol* 1954;6(12):731–44.
 - 38. Jerosch-Herold M, Swingen C, Seethamraju RT. Myocardial blood flow quantification with MRI by model-independent deconvolution. *Med Phys* 2002;29(5):886–97.
 - 39. Jerosch-Herold M, Wilke N, Stillman AE. Magnetic resonance quantification of the myocardial perfusion reserve with a Fermi function model for constrained deconvolution. *Med Phys* 1998;25(1):73–84.
 - 40. Jerosch-Herold M. Quantification of myocardial perfusion by cardiovascular magnetic resonance. *J Cardiovasc Magn Reson* 2010;12:57.
 - 41. Chung S, Shah B, Storey P, et al. Quantitative perfusion analysis of first-pass contrast enhancement kinetics: application to MRI of myocardial perfusion in coronary artery disease. *PLoS One* 2016;11(9):e0162067.
 - 42. Kozerke S, Plein S. Accelerated CMR using zonal, parallel and prior knowledge driven imaging methods. *J Cardiovasc Magn Reson* 2008;10:29.
 - 43. Motwani M, Lockie T, Greenwood JP, et al. Accelerated, high spatial resolution cardiovascular magnetic resonance myocardial perfusion imaging. *J Nucl Cardiol* 2011;18(5):952–8.
 - 44. Tsao J, Kozerke S. MRI temporal acceleration techniques. *J Magn Reson Imaging* 2012;36(3):543–60.
 - 45. Weber S, Kronfeld A, Kunz RP, et al. Comparison of three accelerated pulse sequences for semiquantitative myocardial perfusion imaging using sensitivity encoding incorporating temporal filtering (TSENSE). *J Magn Reson Imaging* 2007;26(3):569–79.
 - 46. Kellman P, Derbyshire JA, Agyeman KO, et al. Extended coverage first-pass perfusion imaging using slice-interleaved TSENSE. *Magn Reson Med* 2004;51(1):200–4.
 - 47. Gebker R, Jahnke C, Paetsch I, et al. MR myocardial perfusion imaging with k-space and time broad-use linear acquisition speed-up technique: feasibility study. *Radiology* 2007;245(3):863–71.
 - 48. Pedersen H, Kozerke S, Ringgaard S, et al. *k-t* PCA: temporally constrained *k-t* BLAST reconstruction using principal component analysis. *Magn Reson Med* 2009;62(3):706–16.
 - 49. Schmidt JF, Wissmann L, Manka R, et al. Iterative *k-t* principal component analysis with nonrigid motion correction for dynamic three-dimensional cardiac perfusion imaging. *Magn Reson Med* 2014;72(1):68–79.
 - 50. Ge L, Kino A, Griswold M, et al. Myocardial perfusion MRI with sliding-window conjugate-gradient HYPR. *Magn Reson Med* 2009;62(4):835–9.
 - 51. Ma H, Yang J, Liu J, et al. Myocardial perfusion magnetic resonance imaging using sliding-window conjugate-gradient highly constrained back-projection reconstruction for detection of coronary artery disease. *Am J Cardiol* 2012;109(8):1137–41.
 - 52. Plein S, Ryf S, Schwitter J, et al. Dynamic contrast-enhanced myocardial perfusion MRI accelerated with *k-t* sense. *Magn Reson Med* 2007;58(4):777–85.
 - 53. Maredia N, Radjenovic A, Kozerke S, et al. Effect of improving spatial or temporal resolution on image quality and quantitative perfusion assessment with *k-t* SENSE acceleration in first-pass CMR myocardial

- perfusion imaging. *Magn Reson Med* 2010;64(6):1616–24.
54. Motwani M, Maredia N, Fairbairn TA, et al. High-resolution versus standard-resolution cardiovascular MR myocardial perfusion imaging for the detection of coronary artery disease. *Circ Cardiovasc Imaging* 2012;5(3):306–13.
 55. Motwani M, Jogiya R, Kozerke S, et al. Advanced cardiovascular magnetic resonance myocardial perfusion imaging: high-spatial resolution versus 3-dimensional whole-heart coverage. *Circ Cardiovasc Imaging* 2013;6(2):339–48.
 56. Manka R, Jahnke C, Kozerke S, et al. Dynamic 3-dimensional stress cardiac magnetic resonance perfusion imaging: detection of coronary artery disease and volumetry of myocardial hypoenhancement before and after coronary stenting. *J Am Coll Cardiol* 2011;57(4):437–44.
 57. Jogiya R, Kozerke S, Morton G, et al. Validation of dynamic 3-dimensional whole heart magnetic resonance myocardial perfusion imaging against fractional flow reserve for the detection of significant coronary artery disease. *J Am Coll Cardiol* 2012;60(8):756–65.
 58. Manka R, Paetsch I, Kozerke S, et al. Whole-heart dynamic three-dimensional magnetic resonance perfusion imaging for the detection of coronary artery disease defined by fractional flow reserve: determination of volumetric myocardial ischaemic burden and coronary lesion location. *Eur Heart J* 2012;33(16):2016–24.
 59. Manka R, Wissmann L, Gebker R, et al. Multicenter evaluation of dynamic three-dimensional magnetic resonance myocardial perfusion imaging for the detection of coronary artery disease defined by fractional flow reserve. *Circ Cardiovasc Imaging* 2015;8(5) [pii:e003061].
 60. Jogiya R, Morton G, De Silva K, et al. Ischemic burden by 3-dimensional myocardial perfusion cardiovascular magnetic resonance: comparison with myocardial perfusion scintigraphy. *Circ Cardiovasc Imaging* 2014;7(4):647–54.
 61. Wissmann L, Niemann M, Gotschy A, et al. Quantitative three-dimensional myocardial perfusion cardiovascular magnetic resonance with accurate two-dimensional arterial input function assessment. *J Cardiovasc Magn Reson* 2015;17:108.
 62. Motwani M, Kidambi A, Sourbron S, et al. Quantitative three-dimensional cardiovascular magnetic resonance myocardial perfusion imaging in systole and diastole. *J Cardiovasc Magn Reson* 2014;16:19.
 63. Pilz G, Klos M, Ali E, et al. Angiographic correlations of patients with small vessel disease diagnosed by adenosine-stress cardiac magnetic resonance imaging. *J Cardiovasc Magn Reson* 2008;10:8.
 64. Kawecka-Jaszcz K, Czarnecka D, Olszanecka A, et al. Myocardial perfusion in hypertensive patients with normal coronary angiograms. *J Hypertens* 2008;26(8):1686–94.
 65. Panting JR, Gatehouse PD, Yang GZ, et al. Abnormal subendocardial perfusion in cardiac syndrome X detected by cardiovascular magnetic resonance imaging. *N Engl J Med* 2002;346(25):1948–53.
 66. Stanton T, Marwick TH. Assessment of subendocardial structure and function. *JACC Cardiovasc Imaging* 2010;3(8):867–75.
 67. Kerkpatananipat P, Gandhi SK, Darty SN, et al. Feasibility to detect severe coronary artery stenoses with upright treadmill exercise magnetic resonance imaging. *Am J Cardiol* 2003;92(5):603–6.
 68. Pennell DJ, Underwood SR, Ell PJ, et al. Dipyradomole magnetic resonance imaging: a comparison with thallium-201 emission tomography. *Br Heart J* 1990;64(6):362–9.
 69. Nagel E, Lehmkuhl HB, Bocksch W, et al. Noninvasive diagnosis of ischemia-induced wall motion abnormalities with the use of high-dose dobutamine stress MRI: comparison with dobutamine stress echocardiography. *Circulation* 1999;99(6):763–70.
 70. Hundley WG, Hamilton CA, Thomas MS, et al. Utility of fast cine magnetic resonance imaging and display for the detection of myocardial ischemia in patients not well suited for second harmonic stress echocardiography. *Circulation* 1999;100(16):1697–702.
 71. Schinkel AF, Bax JJ, Boersma E, et al. Assessment of residual myocardial viability in regions with chronic electrocardiographic Q-wave infarction. *Am Heart J* 2002;144(5):865–9.
 72. Baer FM, Voth E, Schneider CA, et al. Comparison of low-dose dobutamine-gradient-echo magnetic resonance imaging and positron emission tomography with [¹⁸F]fluorodeoxyglucose in patients with chronic coronary artery disease. A functional and morphological approach to the detection of residual myocardial viability. *Circulation* 1995;91(4):1006–15.
 73. Kim RJ, Fieno DS, Parrish TB, et al. Relationship of MRI delayed contrast enhancement to irreversible injury, infarct age, and contractile function. *Circulation* 1999;100(19):1992–2002.
 74. Schinkel AF, Poldermans D, Elhendy A, et al. Assessment of myocardial viability in patients with heart failure. *J Nucl Med* 2007;48(7):1135–46.
 75. Kim RJ, Wu E, Rafael A, et al. The use of contrast-enhanced magnetic resonance imaging to identify reversible myocardial dysfunction. *N Engl J Med* 2000;343(20):1445–53.
 76. Baer FM, Theissen P, Schneider CA, et al. Dobutamine magnetic resonance imaging predicts contractile recovery of chronically dysfunctional myocardium after successful revascularization. *J Am Coll Cardiol* 1998;31(5):1040–8.

77. Kaandorp TA, Lamb HJ, van der Wall EE, et al. Cardiovascular MR to access myocardial viability in chronic ischaemic LV dysfunction. *Heart* 2005; 91(10):1359–65.
78. Rehwald WG, Fieno DS, Chen EL, et al. Myocardial magnetic resonance imaging contrast agent concentrations after reversible and irreversible ischemic injury. *Circulation* 2002;105(2):224–9.
79. Bulow H, Klein C, Kuehn I, et al. Cardiac magnetic resonance imaging: long term reproducibility of the late enhancement signal in patients with chronic coronary artery disease. *Heart* 2005;91(9):1158–63.
80. Ibrahim T, Nekolla SG, Hornke M, et al. Quantitative measurement of infarct size by contrast-enhanced magnetic resonance imaging early after acute myocardial infarction: comparison with single-photon emission tomography using Tc99m-sestamibi. *J Am Coll Cardiol* 2005;45(4):544–52.
81. Kwong RY, Chan AK, Brown KA, et al. Impact of unrecognized myocardial scar detected by cardiac magnetic resonance imaging on event-free survival in patients presenting with signs or symptoms of coronary artery disease. *Circulation* 2006;113(23): 2733–43.
82. Kwong RY, Sattar H, Wu H, et al. Incidence and prognostic implication of unrecognized myocardial scar characterized by cardiac magnetic resonance in diabetic patients without clinical evidence of myocardial infarction. *Circulation* 2008;118(10): 1011–20.
83. Wellnhofer E, Olariu A, Klein C, et al. Magnetic resonance low-dose dobutamine test is superior to SCAR quantification for the prediction of functional recovery. *Circulation* 2004;109(18):2172–4.
84. Selvanayagam JB, Kardos A, Francis JM, et al. Value of delayed-enhancement cardiovascular magnetic resonance imaging in predicting myocardial viability after surgical revascularization. *Circulation* 2004;110(12):1535–41.
85. Lauerman K, Niemi P, Hanninen H, et al. Multimodality MR imaging assessment of myocardial viability: combination of first-pass and late contrast enhancement to wall motion dynamics and comparison with FDG PET-initial experience. *Radiology* 2000;217(3): 729–36.
86. Bello D, Shah DJ, Farah GM, et al. Gadolinium cardiovascular magnetic resonance predicts reversible myocardial dysfunction and remodeling in patients with heart failure undergoing beta-blocker therapy. *Circulation* 2003;108(16):1945–53.
87. Bleeker GB, Kaandorp TA, Lamb HJ, et al. Effect of posterolateral scar tissue on clinical and echocardiographic improvement after cardiac resynchronization therapy. *Circulation* 2006;113(7): 969–76.
88. Coelho-Filho OR, Seabra LF, Mongeon FP, et al. Stress myocardial perfusion imaging by CMR provides strong prognostic value to cardiac events regardless of patient's sex. *JACC Cardiovasc Imaging* 2011;4(8):850–61.
89. Wilke N, Jerosch-Herold M, Wang Y, et al. Myocardial perfusion reserve: assessment with multislice, quantitative, first-pass MR imaging. *Radiology* 1997;204(2):373–84.
90. Doyle M, Fuisz A, Kortright E, et al. The impact of myocardial flow reserve on the detection of coronary artery disease by perfusion imaging methods: an NHLBI WISE study. *J Cardiovasc Magn Reson* 2003;5(3):475–85.
91. Kelm M, Strauer BE. Coronary flow reserve measurements in hypertension. *Med Clin North Am* 2004; 88(1):99–113.
92. Laine H, Raitakari OT, Niinikoski H, et al. Early impairment of coronary flow reserve in young men with borderline hypertension. *J Am Coll Cardiol* 1998;32(1):147–53.
93. Weismuller S, Czernin J, Sun KT, et al. Coronary vasodilatory capacity is impaired in patients with dilated cardiomyopathy. *Am J Card Imaging* 1996;10(3): 154–62.
94. Ingkanisorn WP, Kwong RY, Bohme NS, et al. Prognosis of negative adenosine stress magnetic resonance in patients presenting to an emergency department with chest pain. *J Am Coll Cardiol* 2006;47(7):1427–32.
95. Kwong RY, Schussheim AE, Rekhraj S, et al. Detecting acute coronary syndrome in the emergency department with cardiac magnetic resonance imaging. *Circulation* 2003;107(4):531–7.
96. Steel K, Broderick R, Gandla V, et al. Complementary prognostic values of stress myocardial perfusion and late gadolinium enhancement imaging by cardiac magnetic resonance in patients with known or suspected coronary artery disease. *Circulation* 2009;120(14):1390–400.
97. Jahnke C, Nagel E, Gebker R, et al. Prognostic value of cardiac magnetic resonance stress tests: adenosine stress perfusion and dobutamine stress wall motion imaging. *Circulation* 2007;115(13):1769–76.
98. Pilz G, Jeske A, Klos M, et al. Prognostic value of normal adenosine-stress cardiac magnetic resonance imaging. *Am J Cardiol* 2008;101(10): 1408–12.